

Lanthanum–Indium Oxsulfide as a Visible Light Driven Photocatalyst for Water Splitting

Kiyonori Ogisu,¹ Akio Ishikawa,¹ Kentaro Teramura,¹ Kenji Toda,² Michikazu Hara,³ and Kazunari Domen^{*1}

¹Department of Chemical System Engineering, The University of Tokyo, 7-3-1 Hongo, Bunkyo-ku, Tokyo 113-8656

²Graduate School of Science and Technology, Niigata University, 8050 Ikarashi Ninocho, Niigata 950-2181

³Materials and Structures Laboratory, Tokyo Institute of Technology, 4259 Nagatuta, Midori-ku, Yokohama 226-8503

(Received April 9, 2007; CL-070380; E-mail: domen@chemsys.t.u-tokyo.ac.jp)

La–In-based oxsulfide is demonstrated to act as a photocatalyst for the reduction of H^+ to H_2 and the oxidation of H_2O to O_2 in the presence of sacrificial reagents under visible light ($420 \leq \lambda \leq 480 \text{ nm}$). Loading with IrO_2 is effective for promoting O_2 evolution, while Pt is effective as a cocatalyst for H_2 evolution.

Certain sulfides, such as CdS ^{1,2} and $(\text{AgIn})_x\text{Zn}_{2(1-x)}\text{S}_2$,³ exhibit good absorption in the visible-light region^{4–6} and display activity for the photoreduction of H^+ to H_2 in the presence of an electron donor such as S^{2-} and SO_3^{2-} . However, sulfides are generally unstable in water oxidation to form O_2 because the S^{2-} anions are sensitive to oxidation by photogenerated holes.^{7,8} Recently, $\text{Ln}_2\text{Ti}_2\text{S}_2\text{O}_5$ ($\text{Ln} = \text{Pr–Er}$) oxsulfides have been demonstrated to act as stable photocatalysts for both H^+ reduction and the oxidation of H_2O to O_2 .^{9,10} In the present study, La–In oxsulfide with d^{10} electric configuration is investigated as another potential photocatalytic material for water splitting under visible light.

Following the example of Kabbour et al.,¹¹ the preparation of LaInS_2O was attempted in this study by heating a mixture of La_2S_3 , La_2O_3 , and In_2S_3 at a stoichiometric molar ratio ($\text{La}_2\text{S}_3:\text{La}_2\text{O}_3:\text{In}_2\text{S}_3 = 1:2:3$) in a sealed quartz tube under vacuum at temperatures of 873–1273 K for 6–24 h.¹¹ In this study, we henceforth report the sample obtained at 1073 K for 12 h, which showed the highest photocatalytic activities among all prepared samples. The sintered samples were then ground and heated at 573 K for 1 h in air to remove absorbed sulfur⁹ to yield a yellow powder. The crystal structure of the resulting material was examined by powder X-ray diffraction (XRD) using a Rigaku Geigerflex RAD-B instrument with $\text{Cu K}\alpha$ radiation. Ultraviolet–visible diffuse reflectance (UV–vis DR) spectra were obtained using a Jasco V-560 spectrometer. Photoreduction of H^+ to H_2 and photooxidation of H_2O to O_2 in the presence of sacrificial reagents were carried out in a Pyrex reaction vessel connected to a gas-circulation system. H_2 evolution was examined using an aqueous solution (200 mL) containing 0.1 g of the oxsulfide loaded with Pt metals by in situ photodeposition, and 0.01 M Na_2S and 0.01 M Na_2SO_3 as sacrificial electron donors. O_2 evolution was examined using an aqueous 0.01 M AgNO_3 solution containing 0.1 g of the oxsulfide loaded with IrO_2 by the impregnation method with Na_2IrCl_6 solution and then the treatment in air at 573 K for 1 h. La_2O_3 was used as a buffer material to maintain the pH of the solution at 7–8.

The reaction solution was evacuated several times to remove air and then irradiated under visible light using a 300-W Xe lamp with a cutoff filter ($\lambda > 420 \text{ nm}$) to eliminate UV light and water filter to remove infrared light.

Most of the crystalline peaks produced by the present sam-

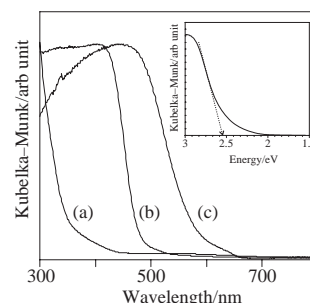


Figure 1. UV–vis diffuse reflectance spectra for (a) LaInO_3 , (b) La–In oxsulfide, and (c) $\text{Sm}_2\text{Ti}_2\text{S}_2\text{O}_5$.⁹

ples matched those for LaInS_2O reported by Kabbour et al.¹¹ Yet, the structural detail of the LaInS_2O phase is unknown. Given the presence of In_2O_3 in the XRD pattern, the oxsulfide obtained by the present preparation procedure is considered to be a mixture of In-poor $\text{La}_5\text{In}_3\text{S}_9\text{O}_3$ and minor impurity phases, most likely $\text{La}_{1.33}\text{In}_{1.33}\text{S}_4$ ¹² and LaIn_2S_4 .¹³ As a single-phase $\text{La}_5\text{In}_3\text{S}_9\text{O}_3$ powder sample could not be obtained from starting materials with a nominal composition of $\text{La}:\text{In} = 5:3$, $\text{La}_5\text{In}_3\text{S}_9\text{O}_3$ may exist in the present samples as a metastable phase in an overall In-rich ($\text{La}:\text{In} = 1:1$) system. Therefore, the prepared samples containing those phases henceforth are denoted as La–In oxsulfide.

Figure 1 shows the UV–vis DR spectra for the present La–In oxsulfide and LaInO_3 . For comparison, UV–vis DR spectrum of $\text{Sm}_2\text{Ti}_2\text{S}_2\text{O}_5$ is also shown. Plane-wave-based density function theory (DFT) calculations have suggested that the valence band (E_{VB}) of $\text{Sm}_2\text{Ti}_2\text{S}_2\text{O}_5$ is made up of the $\text{O}2p$ and $\text{S}3p$ hybridized orbitals and the conduction band (E_{CB}) consists of $\text{Ti}3d$; as a result, $\text{Sm}_2\text{Ti}_2\text{S}_2\text{O}_5$ has a smaller band-gap energy ($\approx 2.1 \text{ eV}$) compared with that of $\text{Sm}_2\text{Ti}_2\text{O}_7$ ($\approx 3.5 \text{ eV}$).⁹ Similarly, the E_{VB} of the La–In oxsulfide appears to consist of the $\text{O}2p$ and $\text{S}3p$ orbitals. On the other hand, the E_{CB} of La–In oxsulfide and LaInO_3 in both cases would be composed of hybridized $\text{In}5s5p$ orbitals.¹⁴ Accordingly, the La–In oxsulfide has a smaller band-gap energy ($\approx 2.6 \text{ eV}$) than LaInO_3 ($\approx 4.1 \text{ eV}$).

Figure 2 shows the time course of repeated H_2 evolution over La–In oxsulfide loaded with 1.0 wt % Pt under visible-light irradiation ($\lambda > 420 \text{ nm}$) in the presence of $\text{Na}_2\text{S–Na}_2\text{SO}_3$. The reaction system was evacuated every 5 h. In the early stage of the reaction (2 h), H_2PtCl_6 was reduced to Pt as an H_2 evolution promoter on the catalyst surface. The rate of H_2 evolution, however, remained essentially stable after this induction period. The XRD pattern of the catalyst after the H_2 evolution reaction was the same as before the reaction. The Pt-loaded La–In oxsulfide therefore functions as a stable photocatalyst for the reduction of H^+ to H_2 under visible-light irradiation.

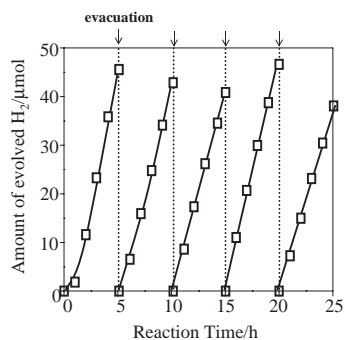


Figure 2. Time course of repeated H_2 evolution over La-In oxysulfide (Pt-loaded catalyst, 0.1 g; 0.01 M Na_2S –0.01 M Na_2SO_3 solution, 200 mL).

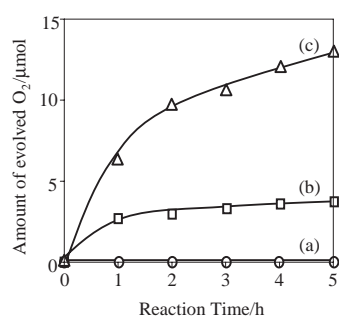


Figure 3. Time course of O_2 evolution over (a) CdS, (b) La-In oxysulfide, and (c) 2 wt % IrO_2 /La-In oxysulfide under visible-light irradiation ($\lambda > 420$ nm) (catal., 0.1 g; 0.01 M AgNO_3 solution, 200 mL; La_2O_3 , 0.2 g).

Figure 3 shows the time courses of O_2 evolution over bare and IrO_2 -loaded La-In oxysulfide, and over CdS for comparison. O_2 evolution was not observed over CdS owing to the photodecomposition of CdS by photogenerated holes. In contrast, over the bare La-In oxysulfide, O_2 evolution was observed immediately with the onset of irradiation. Loading with 2 wt % IrO_2 increased the evolution rate by approximately three-fold, indicating that IrO_2 is an effective O_2 evolution promoter for the La-In oxysulfide. After an initial period (1 h), the rate of O_2 evolution decreased over time owing to the deposition of metallic silver on the surface of the catalyst.

Figure 4 shows the relationship between the H_2 and O_2 evolution rates and the cutoff wavelength of incident light. The steady rate of H_2 evolution and the initial rate of O_2 evolution decreased with increasing cutoff wavelength, confirming the position of the absorption edge of the La-In oxysulfide and the procession of these photocatalytic reactions via band-gap transitions. No O_2 evolution was observed under visible-light irradiation with longer wavelength than 500 nm because of our detection limit to be $\approx 0.1 \mu\text{mol h}^{-1}$.

The apparent quantum efficiencies (QE)¹⁵ of H_2 and O_2 for La-In oxysulfide (Fig. 2 and Fig. 3b) were estimated to be ≈ 0.2 and $\approx 0.1\%$, respectively, indicating that La-In oxysulfide exhibited superior QE for H_2 evolution and lower QE for O_2 evolution compared to those of $\text{Sm}_2\text{Ti}_2\text{S}_2\text{O}_5$ [QE: 0.1% (H_2), 0.2% (O_2)].⁹ Although many factors should affect photocatalytic activity, it seems that E_{CB} of $\text{In}5s5p$ orbitals with large dispersion¹⁴ mainly led to the higher QE of H_2 evolution and the purity

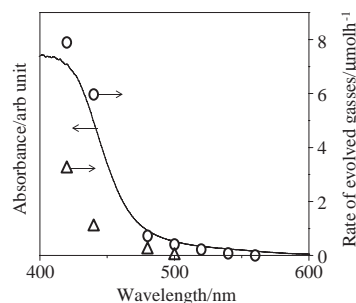


Figure 4. Dependence of rate of H_2 and O_2 evolution on cutoff wavelength of incident light, and UV-vis DR spectrum of La-In oxysulfide. Circles denote H_2 evolution (1 wt % Pt-loaded catal., 0.1 g; 0.01 M Na_2S –0.01 M Na_2SO_3 solution), and triangles denote O_2 evolution (2 wt % IrO_2 -loaded catal., 0.1 g; 0.01 M AgNO_3 solution, La_2O_3 , 0.2 g).

of La-In oxysulfide containing sulfide phases influenced the QE for O_2 evolution.

La-In oxysulfide was demonstrated to catalyze the reduction of H^+ to H_2 and the oxidation of H_2O to O_2 under visible-light irradiation in the presence of a sacrificial electron donor (Na_2S – Na_2SO_3) or acceptor (Ag^+), respectively. This oxysulfide, with a band gap of 2.6 eV, was thus confirmed to be a photocatalyst with reduction and oxidation abilities, having conduction and valence bands at suitable potentials for the reduction of H^+ and oxidation of H_2O . O_2 evolution was effectively enhanced by loading with IrO_2 , while Pt proved to be suitable as a cocatalyst for H_2 evolution.

References

- N. Bühler, K. Meier, J.-F. Reber, *J. Phys. Chem.* **1984**, *88*, 3261.
- M. Matsumura, S. Furukawa, Y. Saho, H. Tsubomura, *J. Phys. Chem.* **1985**, *89*, 1327.
- I. Tsuji, H. Kato, H. Kobayashi, A. Kudo, *J. Am. Chem. Soc.* **2004**, *126*, 13406.
- K. Domen, J. N. Kondo, M. Hara, T. Takata, *Bull. Chem. Soc. Jpn.* **2000**, *73*, 1307.
- A. Kudo, H. Kato, I. Tsuji, *Chem. Lett.* **2004**, *33*, 1534.
- J. Sato, N. Saito, H. Nishiyama, Y. Inoue, *J. Phys. Chem. B* **2003**, *107*, 7965.
- R. Williams, *J. Chem. Phys.* **1960**, *32*, 1505.
- H. Gerischer, *J. Electroanal. Chem. Interfacial Electrochem.* **1975**, *58*, 263.
- A. Ishikawa, T. Takata, J. N. Kondo, M. Hara, H. Kobayashi, K. Domen, *J. Am. Chem. Soc.* **2002**, *124*, 13547.
- A. Ishikawa, T. Takata, T. Matsumura, J. N. Kondo, M. Hara, H. Kobayashi, K. Domen, *J. Phys. Chem. B* **2004**, *108*, 2637.
- H. Kabbour, L. Cario, Y. Moëlo, A. Meerschaut, *J. Solid State Chem.* **2004**, *177*, 1053.
- A. Likforman, M. Cuittard, *Acta Crystallogr., Sect. C* **1993**, *49*, 1270.
- S. A. Amirov, N. A. Shnulin, G. G. Guseinov, S. Kh. Mamedov, *Kristallografiya* **1984**, *29*, 787.
- J. Sato, H. Kobayashi, Y. Inoue, *J. Phys. Chem. B* **2003**, *107*, 7970.
- Quantum efficiency values were calculated with using the coefficients (H_2 : 2, O_2 : 4), steady H_2 or initial O_2 evolution rate, the rate of absorption of incident photons [$\text{Sm}_2\text{Ti}_2\text{S}_2\text{O}_5$: 8.6×10^{21} photons h^{-1} at $440 \leq \lambda \leq 650$ nm, La-In oxysulfide: 7.4×10^{21} photons h^{-1} at $420 \leq \lambda \leq 600$ nm].